A Passive 2-DOF Walker: Hunting for Gaits Using Virtual Holonomic Constraints

Leonid B. Freidovich, *Member, IEEE*,
Uwe Mettin, *Student Member, IEEE*,
Anton S. Shiriaev, *Member, IEEE*, and Mark W. Spong, *Fellow, IEEE*

***Abstract*—A planar compass-like biped on a shallow slope is one of the simplest models of a passive walker. It is a 2-degree-of-freedom (DOF) impulsive mechanical system that is known to possess periodic solutions reminiscent of human walking. Finding such solutions is a challenging computational task that has attracted many researchers who are motivated by various aspects of passive and active dynamic walking. We propose a new approach to find stable as well as unstable hybrid limit cycles without integrating the full set of differential equations and, at the same time, without approximating the dynamics. The procedure exploits a time-independent representation of a possible periodic solution via a virtual holonomic constraint. The description of the limit cycle obtained in this way is useful for the analysis and characterization of passive gaits as well as for design of regulators to achieve gaits with the smallest required control efforts. Some insights into the notion of hybrid zero dynamics, which are related to such a description, are presented as well.**

***Index Terms*—Limit cycles, underactuated mechanical systems, virtual holonomic constraints, walking robots.**

I. Introduction

The study of passive walking devices is a fascinating field. It has especially attracted the attention of researchers in the robotics and control communities after McGeer's seminal paper [19], which was published in 1990. After that, there was a series of publications (see, e.g., [4], [8], [9], [13], [16], [17], and [24]) that proposed and reported how to find and analyze passive gaits for various walking devices. The main difficulty in searching for stable limit cycles is that they usually have comparably small regions of attraction in the state space. Commonly, the search for initial conditions that yield cycles is carried out by numerical computation routines, sometimes using approximations of the dynamics in order to obtain good initial guesses.

The main contribution of this paper is a new approach to find and characterize hybrid limit cycles, which results in a numerical procedure that allows reduction of the computational burden without involving any approximation of the dynamical model. Our arguments can be equally applied to find both stable and unstable cycles.

The key idea of the paper is to explore a special but generic change of coordinates that can always be used to parameterize any nontrivial hybrid periodic solution of the walker dynamics. We avoid looking for explicit dependence on time but instead search for relations between the generalized coordinates [1], [10] that should be valid along a cycle. Such relations are called virtual holonomic constraints [22], [26] and are rapidly becoming increasingly broadly used for periodic motion planning and orbital feedback stabilization for mechanical systems with and without impacts (see, e.g., [21] and [26] and references therein).

In this paper, we demonstrate the usefulness of the concept on a standard benchmark example: a planar two-link walker that is commonly known as a compass-gait biped. Finding stable gaits for this particular system has attracted many researchers who have been motivated by various aspects of passive and active dynamic walking (see, e.g., [6], [7], [11], [14], [18] and [20] and references therein). Here, we show how to use virtual holonomic constraints for analysis of a passive system with multiple degrees of freedom (DOFs).

II. Problem Formulation

A search for a stable walking gait consists of first finding initial conditions in the state space that yield hybrid limit cycles for the hybrid and nonlinear dynamics of the walking robot for a given slope of the ground surface and, second, verifying its stability. Both tasks are nontrivial and are related to the more or less classical problem of analytical mechanics: how to integrate nonlinear dynamical equations. A typical approach for solving both problems is to proceed with heavy numerical simulations of the system dynamics rather than attempt analytical arguments. In support of this opinion more than a decade ago, Goswami *et al.* wrote in their seminal paper [9], "[. . .] the analytical demonstration of the existence of a limit cycle, its local orbital stability, and the analytical procedure to find it still remains a challenge." Since then, there has been a little if any progress in deriving such analytical arguments.

In this paper, we suggest analytical and constructive steps that allow the reduction of the number of parameters to be found in the search for suitable initial conditions and the number of differential equations that must be integrated numerically. However, the main contribution is not the reduction of the computational burden but in a new way of characterizing limit cycles. The core of the paper is an almost trivial observation that a periodic gait of a walking machine, if it exists, can be characterized by a certain synchronization between its generalized coordinates. Basically, we suggest searching for such relations rather than attempting to identify a periodic trajectory directly. It is worth noting that finding such a relation among the generalized coordinates for a numerically computed cycle is a highly nontrivial task [26, Ch. 6] and that knowledge of such a function allows not only verifying stability of the cycle analytically but obtaining an analytical expression for the Poincaré first-return map as well [5].

Such arguments, which are elaborated for computing hybrid limit cycles of the planar compass-gait biped, are presented as follows. For simplicity, we search only for symmetric walking gaits, i.e., the gaits of interest are characterized by a periodic sequence of two identical steps of the respective legs. Given a walking gait, if T_i is the time interval between two consecutive impacts with indexes i and $(i+1)$, and T_p is the period of the gait cycle, then for a symmetric gait cycle,[1] $T_p = T_i + T_{i+1}$ with $T_i = T_{i+1} = T_p/2$.

Manuscript received February 6, 2009. First published September 1, 2009; current version published October 9, 2009. This paper was recommended for publication by Associate Editor F. Lamiraux and Editor W. K. Chung upon evaluation of the reviewers' comments. This work was supported in part by the Kempe Foundation, in part by the Swedish Research Council under Grant 2005-4182 and Grant 2008-4369, and in part by the U.S. National Science Foundation under Grant CMMI-0510119. This paper was presented in part at the 47th IEEE Conference on Decision and Control.

L. B. Freidovich and U. Mettin are with the Department of Applied Physics and Electronics, Umeå University, SE-901 87 Umeå, Sweden (e-mail: leonid.freidovich@tfe.umu.se).

A. S. Shiriaev is with the Department of Applied Physics and Electronics, Umeå University, SE-901 87 Umeå, Sweden, and also with the Department of Engineering Cybernetics, Norwegian University of Science and Technology, NO-7491 Trondheim, Norway.

M. W. Spong is with Erik Jonsson School of Engineering and Computer Science, University of Texas, Dallas, TX 75080-3021 USA.

Color versions of one or more of the figures in this paper are available online at http://ieeexplore.ieee.org.

Digital Object Identifier 10.1109/TRO.2009.2028757

[1] If a walking gait is not symmetric and shaped by k consecutive intervals of continuous dynamics (i.e., of periodicity k), then the period of the gait is $T_p = T_i + T_{i+1} + \cdots + T_{i+k}$. It turns out that for the proposed method, searching for walking gaits of periodicity $k \geq 2$ and for symmetric gaits are problems of the same complexity that can be solved by similar arguments.

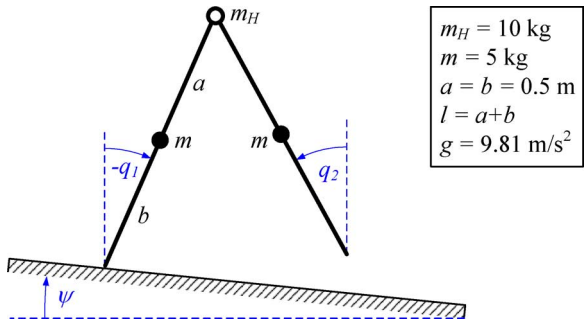

Fig. 1. Schematic of the compass-gait biped on a shallow slope ψ. Here, q_1 and q_2 describe the absolute angular positions of the stance leg and the swing leg, respectively. On the right, physical parameters of the compass-gait robot are listed.

III. Hybrid Dynamics of the Compass-Gait Biped

Let us consider a two-link passive compass-gait biped robot, which is schematically shown in Fig. 1.

Under certain conditions [9], the dynamics of the robot can be described [9], [13], [25] by the following system of Euler–Lagrange equations with impulse effects [3], [10], [26]:

$$\begin{aligned} &p_1\ddot{q}_1 - p_2\cos(q_1-q_2)\ddot{q}_2 - p_2\sin(q_1-q_2)\dot{q}_2^2 - p_4\sin q_1 = 0 \\ &p_3\ddot{q}_2 - p_2\cos(q_1-q_2)\ddot{q}_1 + p_2\sin(q_1-q_2)\dot{q}_1^2 + p_5\sin q_2 = 0 \\ &\qquad \text{as long as} \quad q \notin \mathcal{S} \\ &q_1^+ = q_2^-,\ q_2^+ = q_1^- \quad \text{and} \quad \dot{q}^+ = P_q(q^-)\,\dot{q}^- \\ &\qquad \text{whenever} \quad q^- \in \mathcal{S} \end{aligned} \tag{1}$$

where $q = [q_1,\ q_2]^T$ is the vector of generalized coordinates. Here, the coefficients are defined by the physical parameters of the robot as follows: $p_1 = (m_H + m)l^2 + ma^2$, $p_2 = mlb$, $p_3 = mb^2$, $p_4 = (m_H l + mb + ml)g$, $p_5 = mbg$; for the slope ψ of the walking surface, the impact surface is

$$\mathcal{S} = \left\{ q \in \mathbb{R}^2 : H(q) = \cos(q_1 + \psi) - \cos(q_2 + \psi) = 0 \right\}. \tag{2}$$

The impulse effects[2] are described by the reset map

$$P_q = \begin{bmatrix} p_1 - p_2 c_{12}^- & p_3 - p_2 c_{12}^- \\ -p_2 c_{12}^- & p_3 \end{bmatrix}^{-1} \begin{bmatrix} p_7 c_{12}^- - p_6 & -p_6 \\ -p_6 & 0 \end{bmatrix} \tag{3}$$

with $p_6 = mab, p_7 = m_H l^2 + 2mal$, and $c_{12}^- = \cos(q_1^- - q_2^-)$, which is attributed to the jump in velocities due to impact [10], [15], [25]; here and before, the abbreviations

$$q^- = \lim_{\tau \to t-} q(\tau) \qquad \text{and} \qquad q^+ = \lim_{\tau \to t+} q(\tau)$$

are used for the states right before and right after the impact time t.

Our goal is to find symmetric walking gaits of the hybrid system (1) with (2) and (3), respectively.

IV. Finding Hybrid Limit Cycles

In the following, we introduce some notation and formulate the common procedure to find limit cycles and present an alternative approach. The latter is the main contribution of the paper and will be discussed later on.

[2]Note that the swing leg of a rigid two-link walker trespasses this surface during one complete step. For our considerations, the compass-gait robot (1) shall experience impact only when a heel strike occurs.

A. Notation for the Parameters of a Cycle

Given a shallow slope ψ, a nontrivial symmetric periodic solution of (1) is uniquely defined by the vector of parameters[3] $p_\star = [a,\ b,\ c,\ d,\ e,\ f,\ g,\ h,\ T]^T \in \mathbb{R}^9$, which consisted of the half-period $T = T_p/2 > 0$ and the following eight constants, which denote the initial and final states:

$$\begin{aligned} q_\star(0+) &= [q_{1\star}(0+),\ q_{2\star}(0+)]^T = [a,\ e]^T \\ \dot{q}_\star(0+) &= [\dot{q}_{1\star}(0+),\ \dot{q}_{2\star}(0+)]^T = [b,\ f]^T \\ q_\star(T-) &= [q_{1\star}(T-),\ q_{2\star}(T-)]^T = [c,\ g]^T \\ \dot{q}_\star(T-) &= [\dot{q}_{1\star}(T-),\ \dot{q}_{2\star}(T-)]^T = [d,\ h]^T. \end{aligned} \tag{4}$$

Five algebraic relations among these eight parameters can be obtained using the fact that the jump of the states due to impact is described by algebraic relations (2) and (3); the derivations are shown in the Appendix.

B. Procedures to Find Hybrid Limit Cycles

Solving the continuous-time dynamics described by the differential equations in (1), i.e., the four first-order differential equations, on the time interval $0 \le t \le T$, one can obtain the four missing relations to define the parameters a, b, d, and T of the cycle. The period T can also be identified during the numerical integration by the first time a solution hits the surface S given in (2). Therefore, the search for a hybrid cycle is converted into finding a solution (the vector of parameters p_*) for the following problem that can be treated as a standard optimization routine.

Problem 1: Find $a, b, d,$ and T such that $\bar{q}_1(T) = c$, $\bar{q}_2(T) = g$, $\dot{\bar{q}}_1(T) = d$, and $\dot{\bar{q}}_2(T) = h$, with algebraic relations (13) from the Appendix satisfied and $\bar{q}(t)$ being the solution of the differential equations in (1) initiated at $\bar{q}_1(0) = a$, $\bar{q}_2(0) = e$, $\dot{\bar{q}}_1(0) = b$, as well as $\dot{\bar{q}}_2(0) = f$.

Standard optimization Problem 1 is typically solved through numerical integration of the system dynamics.

The following observations allow a different way of proceeding. The continuous subarc of a nontrivial periodic trajectory $q_\star(t)$ for (1), if it exists, is a solution of the differential equations in (1) defined on a finite interval of time. Therefore, the repetitive evolution of the generalized coordinates along the cycle can be specified not only as periodic functions of time $q_\star(t) = q_\star(t + T_p) = [q_{1\star}(t),\ q_{2\star}(t)]^T\ \forall\, t$ but also as functions of a scalar variable that uniquely defines a particular point on the continuous subarc of the cycle $q_{1\star}(t) = \varphi_1(\theta_\star(t))$, $q_{2\star}(t) = \varphi_2(\theta_\star(t))$, for $0 < t < T = T_p/2$. The shape of functions $\varphi_1(\cdot)\,\varphi_2(\cdot)$ depends on the way we parameterize points on the trajectory of the cycle in the state space of the walker, but these functions are clearly unique for each parameterization.

If we assume that the new variable $\theta_\star$ is one of the generalized coordinates, say the coordinate of stance leg, then the reparameterization results in a new representation

$$q_{1\star}(t) = \theta_\star(t), \quad q_{2\star}(t) = \varphi(\theta_\star(t)), \quad \text{for} \quad 0 < t < T \tag{5}$$

of the continuous subarc of the cycle between two consecutive impacts. The scalar functions $\theta_\star(\cdot)$ and $\varphi(\cdot)$ are unknown. To derive equations with respect to these variables, we can use the dynamics of the robot, i.e., substitute

$$q_1 = \theta, \qquad q_2 = \varphi(\theta) \tag{6}$$

[3]The parameters a, b, and g here are not related to the notation for the physical lengths and the gravitational constant given in Fig. 1. The physical parameters are not to be used anywhere in the rest of the paper.

into the Euler–Lagrange equations in (1), and collect similar terms. The next two second-order differential equations for the variable θ are obtained from straightforward computations

$$\alpha_1(\theta)\frac{d^2}{dt^2}\theta + \beta_1(\theta)\left[\frac{d}{dt}\theta\right]^2 + \gamma_1(\theta) = 0 \tag{7}$$

$$\alpha_2(\theta)\frac{d^2}{dt^2}\theta + \beta_2(\theta)\left[\frac{d}{dt}\theta\right]^2 + \gamma_2(\theta) = 0 \tag{8}$$

where $\alpha_1(\theta) = -p_2\cos(\theta-\varphi(\theta))\varphi'(\theta) + p_1, \beta_1(\theta) = -p_2\sin(\theta-\varphi(\theta))(\varphi'(\theta))^2 - p_2\cos(\theta-\varphi(\theta))\varphi''(\theta), \gamma_1(\theta) = -p_4\sin(\theta), \alpha_2(\theta) = -p_2\cos(\theta-\varphi(\theta)) + p_3\varphi'(\theta), \beta_2(\theta) = p_2\sin(\theta-\varphi(\theta)) + p_3\varphi''(\theta)$, and $\gamma_2(\theta) = p_5\sin(\varphi(\theta))$.

In a similar way, for a system with $n \geq 2$ DOF and $0 \leq m \leq n-2$ control inputs, modeling continuous-in-time dynamics of an underactuated walker, one would obtain exactly $(n-m)$ second-order differential equations with the same structure, coefficients of which would depend on $(n-1)$ unknown functions and their two derivatives. These functions describe synchronization among the generalized coordinates along a periodic trajectory and are known as virtual holonomic constraint; see, e.g., [21] and [26]. The fact that each of these second-order differential equations is integrable [23] and that they possess a common solution allows set of new differential equations for the unknown functions to be obtained. This is exactly what is done in the Appendix for the 2-DOF system with 0 control inputs at hand.

Searching for a limit cycle in terms of $\theta_\star(t)$ and $\varphi(\theta_\star)$, instead of $q_{1\star}(t)$ and $q_{2\star}(t)$, results in some numerical simplifications and in the following alternative procedure, which is developed in the Appendix.

Problem 2: Find a and b such that $\bar{\varphi}(c) = g$ and $\bar{\varphi}'(c) = h/d$ with algebraic relations (13) and (18) from the Appendix satisfied and $\bar{\varphi}(\theta)$ being the solution of the differential equation

$$\varphi''(\theta_\star) = f_0\left(a, b, \theta_\star, \varphi(\theta_\star), \varphi'(\theta_\star)\right) \tag{9}$$

which is initiated at $\bar{\varphi}(a) = e$ and $\bar{\varphi}'(a) = f/b$, where the expression for the right-hand side is given in the Appendix.

Solving Problem 2 is computationally simpler than solving Problem 1 since the number of differential equations is reduced, as is the number of free parameters.

Proposition 1: The set of solutions for Problem 2 contains all the solutions of Problem 1.

The *proof* of sufficiency to solve Problem 2 trivially follows from inspecting the derivations in the Appendix. The lack of necessity is, roughly speaking, due to the fact that synchronization relations do not take into account the fact that the negative velocities imply decreasing positions. In fact, half of the solutions for Problem 2 have been found to be extraneous in our numerical search, the results of which being reported shortly.

V. Discussion on Virtual Holonomic Constraints

Prior to presenting a description of the numerical results, let us make a few comments.

It is seen that passing from Problem 1 to Problem 2, we have achieved reduction in the computational burden in half for our model for the compass-gait walker. What is the trick? Eliminating one differential equation and one parameter is the result of searching for a solution in the form without explicit dependence on time. Additionally, it allows the exploitation of the fact that the total energy [cf., the conserved quantity (16)] depends on the synchronization function $\varphi(\theta)$ and its two derivatives point-wise and not in a functional way through integration. Both the number of parameters and the order of the system of the differential equations needed to be solved are further reduced by one. Note that reduction of the order for a mechanical system using a conserved quantity is, in general, an unsolved problem. The difficulty here is the fact that if one wants to use the energy as one of the states for a mechanical system, a nontrivial computation of the appropriate complete coordinate transformation is needed.

However, the main contribution is not simplifying the search procedure but obtaining a useful characterization of the limit cycle. It is important to keep in mind that, for instance, gait stability can be analytically verified using the knowledge of the computed virtual holonomic constraint. Namely, knowledge of the function $\varphi(\theta_\star)$ allows the analytical derivation of coefficients of a linear time-periodic impulsive system, known as transverse linearization, the asymptotic stability of which implies exponential orbital stability of the limit cycle (see [5] for details).

Note that finding such a constraint using polynomial approximations from a numerically computed limit cycle is a nontrivial challenge [26, Ch. 6]. Here, for the first time, such a function is computed as a solution of a differential equation, and therefore, it can be easily and accurately calculated.

Other approaches for the analysis of gait stability for the compass-gait biped with and without actuation has been suggested by many researchers (see, e.g., [2], [12], and [26]).

It seems that the most promising application of virtual holonomic constraints approach is using them for stabilization and planning of periodic trajectories by shaping control inputs. Typically, the passive gaits have very small regions of attraction[4] but clearly require no control efforts following the trajectory. Hence, it is an attractive and natural idea to use feedback control for stabilizing a passive unstable gait or for enlarging the region of attraction for a stable one. A recent breakthrough strategy in walking robot control, which is summarized and detailed in [26], uses virtual holonomic constraints together with the notion of invariant hybrid zero dynamics, which has been introduced in [27]. Invariance of hybrid zero dynamics allows significant simplification in the computation of the Poincaré map that can be used to verify stability. We show below that in the absence of shaping control signals, such a simplification of stability assessment is impossible.

The hybrid zero dynamic $\mathcal{Z}$ associated with the synchronization functions $\varphi_\star(\theta)$, which is induced by a periodic solution, is defined as the following subset of the state space of the walker dynamics:

$$\mathcal{Z} = \left\{[q_1, q_2, \dot{q}_1, \dot{q}_2] : q_2 = \varphi_\star(q_1),\ \dot{q}_2 = \left[\frac{d}{dq_1}\varphi_\star(q_1)\right]\dot{q}_1\right\} \tag{10}$$

and in the vicinity of the cycle, it is a 2-D smooth submanifold of the state space.

Lemma 1: For any nontrivial symmetric gait of the compass gait walker (1), the associated hybrid zero dynamics are invariant with respect to the update law due to an impact.

The *proof* is straightforward and uses the following two facts: The switching surface is invariant with respect to the generalized velocities, and the update law is linear in them. It can be readily generalized to the case with arbitrary number of DOFs. Such a generalization of this lemma has been implicitly used in [26], where the property is called impact invariance. The following statement shows that the whole hybrid zero dynamic for a passive gait cycle is generically not invariant.

Proposition 2: For any nontrivial symmetric gait of the compass-gait walker (1), the associated zero dynamics (10) are not invariant

[4]For the example at hand, it can be deduced from the simulation results of Section VI since the stable and unstable limit cycles are close.

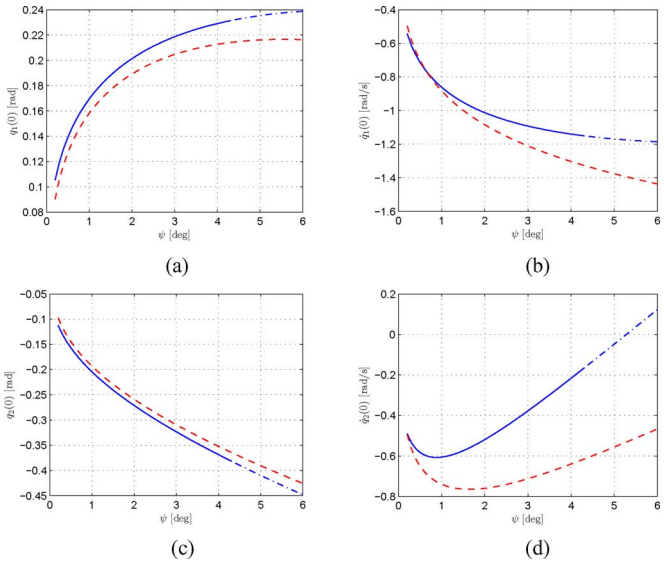

Fig. 2. Initial conditions for the two symmetric gait cycles obtained from analysis. Cycle #2 represented by the dashed line is unstable, while cycle #1 represented by the solid line is exponentially orbitally stable within the interval $\psi \in (0, \sim 4.4)^\circ$ and unstable otherwise. (a) Initial position $q_{\star,1}(0+)$ for the stance leg. (b) Initial velocity $\dot{q}_{\star,1}(0+)$ for the stance leg. (c) Initial position $q_{\star,2}(0+)$ for the swing leg. (d) Initial velocity $\dot{q}_{\star,2}(0+)$ for the swing leg.

with respect to the vector field of the continuous-time dynamics of the walker.

The *proof* is not tightened to the low-dimension dynamics at hand. The statement immediately follows from the definition of generalized coordinates, since invariance of a reduced-order manifold implies reduction of the number of DOFs. Hence, the property called forward invariance in [26, Ch. 6] is generically violated for passive walking gaits.

The conclusion is that the stability of a passive limit cycle cannot be verified using the technique introduced in [27]. It is remarkable to note that even one control input allows the passive hybrid zero-dynamics invariant to be made, as demonstrated in [26, Ch. 6] and [28]. Interestingly enough, forcing the invariance results in a large region of attraction for the example considered here, which, however, does not cover the original one. This leads us to the conjecture that feedback control laws for passive gaits that keep a hybrid zero-dynamic invariant may, at some systems, fail to enlarging the region of attraction.

VI. Numerical Results of Solving Problem 2

Here, we demonstrate the results of solving Problem 2 for finding gaits of the passive walker for the case of the parameters listed in Fig. 1. The shallow slope for the compass-gait biped is chosen in the range of $\psi \in (0, 6]^\circ$, which is about the same interval as discussed in [9]. The initial conditions $q_\star(0+)$ and $\dot{q}_\star(0+)$, as well as the half-period T and the total energy E_0 of the found symmetric gaits for this range of the slope angle, are shown in Figs. 2 and 3 as functions of ψ. As seen, two hybrid limit cycles are found following the proposed arguments. It turns out that these cycles can be distinguished by two different solutions for d, which we expected according to the new procedure developed in the Appendix. For simplicity, the cycles corresponding to the first solution for d will be denoted as cycle #1; the other ones corresponding to the second solution for d will be denoted as cycle #2.

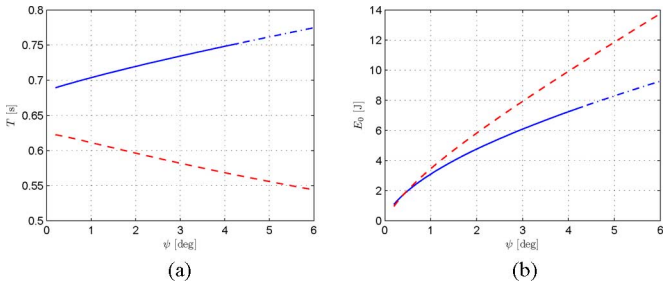

Fig. 3. Half-period and total energy of the two symmetric gait cycles obtained from analysis. The cycle #2 represented by the dashed line is unstable, while the cycle #1 represented by the solid line is exponentially orbitally stable within the interval $\psi \in (0, \sim 4.4)^\circ$ and unstable otherwise. (a) Resulting half-period T. (b) Required total energy E_0.

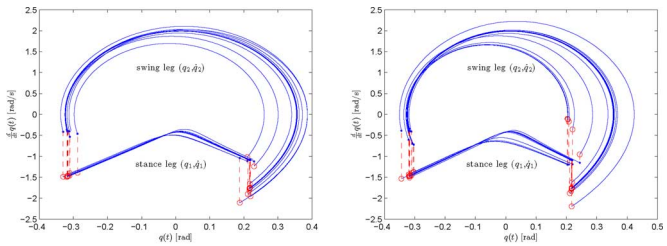

Fig. 4. Simulation results for particular hybrid limit cycles. (a) Convergence to a stable limit cycle #1. (b) Divergence from an unstable limit cycle #2 and convergence to a stable one.

Further numerical studies revealed that the limit cycles #2, represented by the dashed line in Fig. 2, are always unstable.[5] The limit cycles #1, represented by the solid line in Fig. 2, are exponentially orbitally stable within the interval $\psi \in (0, \sim 4.4)^\circ$ and unstable otherwise. For slopes $\psi \geq \sim 4.4^\circ$, one can notice a change in the stability properties caused by bifurcation, which makes the limit cycle unstable. This phenomenon has been already reported in [9] for the compass-gait biped robot. As a result of the bifurcation, the robot exhibits asymmetric gait cycles with $i = 2^n$ steps, where $n = \{1, 2, 3, \ldots\}$ grows with increasing ψ, $\psi \geq \sim 4.4^\circ$. Note that the initial conditions for the two obtained cycles are comparably close to each other, which indicates a small region of attraction for stable limit cycles. Fig. 4 shows some representative simulation results for the following gait cycles:

1) convergence to a stable limit cycle #1 with (this is the same cycle as studied in [25]) $\psi = 2.87^\circ$, $q(0+) = q_\star(0+) + [0.01,\ 0.01]^T$ rad $\approx [0.22689,\ -0.30708]^T$ rad, $\dot{q}(0+) = \dot{q}_\star(0+) + [0.01, 0.01]^T$ rad/s $\approx [-1.07428,\ -0.38728]^T$ rad/s, $T_i = 0.73249$ s for $i \in \mathbb{N}$ after 19 steps;[6]

2) divergence from an unstable limit cycle #2 with $\psi = 2.87^\circ, q(0+) = q_\star(0+) \approx [0.20318,\ -0.30336]^T$ rad, $\dot{q}(0+) = \dot{q}_\star(0+) \approx [-1.19656,\ -0.72051]^T$ rad/s, $T_i = 0.58373$ s for $i \in \mathbb{N}$ and convergence to the stable cycle #1 from 1) after 24 steps.

VII. Conclusion

We have studied the problem of finding hybrid periodic trajectories for a model of the compass-gait biped robot, which consisted of a

[5]To the best of our knowledge, we are the first to find the second set of limit cycles. We have failed to find them using the standard procedure.

[6]Of course, by "convergence," here, we mean that the simulated trajectory becomes close to the cycle with a certain accuracy.

2-DOF continuous-time Euler–Lagrange dynamic and an impact modeled by an instantaneous reset map.

Our approach exploits existence of a geometric relation between the two generalized coordinates along the continuous-time subarc of any periodic trajectory. Our computations lead to a minimization problem, which requires finding two parameters and is based on solving the found second-order differential equation for computation of the target functional. Since there are four first-order differential equations in the description of the dynamics, the burden of numerical computations is reduced by half.

However, the main contribution is the obtained differential equation for the virtual holonomic constraint. Motivated by recent advances in exploiting such constraints for feedback control design, we have also studied applicability of the concept of invariant hybrid zero dynamics. It has been verified that, in general, the corresponding 2-D manifold induced by the periodic trajectory is not invariant.

Finally, we have verified that the proposed computational procedure does work and allows stable as well as unstable limit cycles to be found for a reasonable range of the slopes of the walking surfaces. Some numerical results have been presented.

APPENDIX

RELATIONS AMONG THE PARAMETERS OF A CYCLE

After each step, the robot experiences an impact if it hits the ground, i.e., condition (2) is satisfied. It follows from $q_\star(T_-) \in \mathcal{S}$ that

$$\cos(c+\psi) - \cos(g+\psi) = 0. \tag{11}$$

Lemma 2 (Feasible solutions for the impact surface): The impact surface (2) defines the condition for impulse effects on the hybrid dynamics of the passive compass-like biped robot (1). The parameterized condition (11) gives the following solutions for the parameter c as function of g and ψ, where $q_\star(T-) = [c,\ g]^T$.

1) The solution $c = g$ is extraneous since, in this case, with $\psi = 0$, first, the relation $c = -g$ must hold, and second, the configuration of the robot would be static anyway.

2) Multiple solutions exist in the form $c = -g - 2\,\psi + 2k\pi, k \in \mathbb{Z}$, where, for the range of the slopes $\psi \in (0,\ \pi/2)$, we have feasible configuration angles only in the case when $c \in (-\pi,\ 0),\ \text{for}\ k = 0$, and unfeasible ones otherwise, i.e., $c \notin (-\pi,\ 0),\ \text{for}\ k \neq 0$.

Note that the swing leg of a rigid two-link walker trespasses the impact surface (2) during one complete step. We assume for our considerations that the compass-gait robot experiences an impact only when a heel strike occurs.

The impulse effect (instantaneous change of the states), which is described by the second equation in (1) together with (3), gives the following expressions for the reset states after impact:

$$\underbrace{\begin{bmatrix} a \\ e \end{bmatrix}}_{q_\star(0+)} = \begin{bmatrix} 0 & 1 \\ 1 & 0 \end{bmatrix} \underbrace{\begin{bmatrix} c \\ g \end{bmatrix}}_{q_\star(T-)} = \begin{bmatrix} g \\ c \end{bmatrix}$$

and

$$\underbrace{\begin{bmatrix} b \\ f \end{bmatrix}}_{\dot{q}_\star(0+)} = P_q\left(\underbrace{\begin{bmatrix} c \\ g \end{bmatrix}}_{q_\star(T-)}\right) \underbrace{\begin{bmatrix} d \\ h \end{bmatrix}}_{\dot{q}_\star(T-)}. \tag{12}$$

Solving the system of five algebraic equations (11) and (12) in terms of a, b, and d, one obtains

$$g = a, \quad c = e = -a - 2\,\psi, \quad f = \frac{b\cos(2a+2\psi)\,p_2 - p_6 d}{p_3}$$

$$h = \frac{d(p_3 p_7 - p_6 p_2) - b(p_3 p_1 - p_2^2\cos(2a+2\psi))}{p_3 p_6}\cos(2a+2\psi). \tag{13}$$

APPENDIX

HUNTING FOR CYCLES USING VIRTUAL HOLONOMIC CONSTRAINTS

A useful observation is that the second-order nonlinear differential equations (7) and (8) can be integrated, independent of the coefficient functions, as long as $\alpha(\theta) \neq 0$.

Lemma 3 (Reduced energy): Along any solution $\theta(t)$ of the nonlinear system

$$\alpha(\theta)\,\ddot{\theta} + \beta(\theta)\,\dot{\theta}^2 + \gamma(\theta) = 0 \tag{14}$$

the energy function, if well defined for some constant x

$$E_x(\theta,\dot{\theta}) = \underbrace{\frac{1}{2}\exp\left\{\int_x^\theta \frac{\beta(\tau)}{\alpha(\tau)}d\tau\right\}}_{\Psi_x(\theta)}\dot{\theta}^2 + \underbrace{\int_x^\theta \frac{\gamma(\tau)}{\alpha(\tau)}\Psi_x(\tau)d\tau}_{\Pi_x(\theta)} \tag{15}$$

preserves its value $E_x(\theta(t),\dot{\theta}(t)) \equiv E_x(\theta(0),\dot{\theta}(0))$. In particular, $E_x(\theta(0+),\dot{\theta}(0+)) = E_x(\theta(T-),\dot{\theta}(T-))$ for the time moments right after an impact and right before the next impact.

See the next section of the Appendix for derivation of (15).

Both (7) and (8) are in the form (14); therefore, they have two energies (15), irrespective of the particular form of the unknown function $\varphi(\cdot)$. Keeping in mind that dynamics of the walker is not completely integrable, the presence of two conserved quantities for (7) and (8) is indeed surprising. The explanation for this apparent contradiction is that the conserved quantities are not true first integrals of the system and are solution-dependent.

It is worth observing that any linear combination of (7) and (8) with θ-dependent weights $\mu_1(\theta)$ and $\mu_2(\theta)$ has the form of (14): $(\mu_1(\theta)\alpha_1(\theta) + \mu_2(\theta)\alpha_2(\theta))\,\ddot{\theta} + (\mu_1(\theta)\beta_1(\theta) + \mu_2(\theta)\beta_2(\theta))\,\dot{\theta}^2 + (\mu_1(\theta)\gamma_1(\theta) + \mu_2(\theta)\gamma_2(\theta)) = 0$ and is integrable, while the integral of the last equation is not the sum of integrals of the summands (7) and (8). For instance, with the weights $\mu_1(\theta) = \theta, \mu_2(\theta) = \phi(\theta)$, one restores the true energy of the Euler–Lagrange system (1), i.e., $E(q,\dot{q})$, when the generalized coordinates satisfy the relations (6), i.e.,

$$\begin{aligned} E(q,\dot{q})\big|_{\left\{q_1=\theta, q_2=\phi(\theta), \dot{q}_1=\dot{\theta}, \dot{q}_2=\phi'(\theta)\dot{\theta}\right\}} &= E_0(\theta,\dot{\theta}) \\ &= \left(\frac{p_1}{2} - p_2\,\cos(\theta-\varphi(\theta))\varphi'(\theta) + \frac{p_3}{2}(\varphi'(\theta))^2\right)\dot{\theta}^2 \\ &\quad + p_4\left[\cos(\theta)-1\right] + p_5\left[1-\cos(\varphi(\theta))\right]. \end{aligned} \tag{16}$$

Here, the function $E_0(\cdot)$ is $E_x(\cdot)$ from (15) with $x = 0$.

If the velocities before and after each impact are nonzero, such that $b \neq 0$ and $d \neq 0$, then the boundary conditions (4) can be rewritten in terms of the virtual holonomic constraint (5) as follows:

$$\begin{aligned} &\theta_\star(0) = a, \quad \dot{\theta}_\star(0) = b, \quad \theta_\star(T) = c, \quad \dot{\theta}_\star(T) = d \\ &\varphi(a) = e, \quad \varphi'(a) = \frac{f}{b}, \quad \varphi(c) = g, \quad \varphi'(c) = \frac{h}{d}. \end{aligned} \tag{17}$$

As $E_x(\cdot)$ keeps its value (see Lemma 3), one can substitute the relations (17) into the function (16) in order to obtain another identity among the parameters of the cycle (4)

$$\begin{aligned} E_0(c,d) = E_0(a,b) \overset{(13)}{=} &\frac{p_1 b^2}{2} - p_2\cos(a-e)fb + \frac{p_3 f^2}{2} \\ &+ p_4(\cos(a)-1) + p_5(1-\cos(e)). \end{aligned} \tag{18}$$

As seen, it is a quadratic equation with respect to d; at best, it has two real solutions for given values of a and b.

Reducing the number of parameters to search for in (1) is not the only benefit of using virtual constraints. Let us now reduce the number of differential equations needed to be solved during the search: One can look at the system of differential equations (7) and (8) as a system of algebraic equations for the two unknown functions of time $\dot{\theta}_\star^2(t)$ and $\ddot{\theta}_\star(t)$. To derive a differential equation for the function $\varphi(\cdot)$ used for reparameterization of the desired evolution of generalized coordinates $q_\star(t)$ along the cycle, consider the following two cases.

Case 1: The function $D(\theta) := \beta_1(\theta)\alpha_2(\theta) - \beta_2(\theta)\alpha_1(\theta)$ is separated from zero on a subarc of the cycle, i.e., $D(\theta_\star(t)) \neq 0$ for $0 \leq t_0 \leq t \leq t_1 \leq T$. For this time interval $[t_0, t_1]$, the differential equations (7) and (8) can be solved as algebraic ones[7] w.r.t. $\dot{\theta}_\star(t)$ and $\dot{\theta}_\star(t)$ as follows:

$$\dot{\theta}_\star^2 = \frac{\alpha_2(\theta_\star)\gamma_1(\theta_\star) - \alpha_1(\theta_\star)\gamma_2(\theta_\star)}{\alpha_1(\theta_\star)\beta_2(\theta_\star) - \alpha_2(\theta_\star)\beta_1(\theta_\star)} \tag{19}$$

$$\ddot{\theta}_\star = \frac{\beta_1(\theta_\star)\gamma_2(\theta_\star) - \beta_2(\theta_\star)\gamma_1(\theta_\star)}{\alpha_1(\theta_\star)\beta_2(\theta_\star) - \alpha_2(\theta_\star)\beta_1(\theta_\star)}. \tag{20}$$

The equation (19), in conjunction with the relation on the energy (18), can be rewritten as

$$\dot{\theta}^2 = \frac{E_0(a,b) - p_4(\cos(\theta) - 1) - p_5(1 - \cos(\varphi(\theta)))}{\frac{p_1}{2} - p_2\,\cos(\theta - \varphi(\theta))\,\varphi'(\theta) + \frac{p_3}{2}\,(\varphi'(\theta))^2}. \tag{21}$$

Combining (20) with time derivative of (21) results in the second-order equation for unknown function $\varphi(\cdot)$ given by (9).

Case 2: The function $D(\theta) := \beta_1(\theta)\alpha_2(\theta) - \beta_2(\theta)\alpha_1(\theta)$ is zero on a subarc of the cycle, i.e., $D(\theta_\star(t)) \equiv 0$ for $0 \leq t_0 \leq t \leq t_1 \leq T$. For this time interval, the identity $D(\theta_\star(t)) \equiv 0$ can be used and rewritten as the next differential equation for φ

$$\varphi''(\theta) = -p_2\,\sin(\theta - \varphi(\theta)) \times \frac{(\varphi')^3\,p_3 - p_2\,(\varphi')^2\,\cos(\theta - \varphi) - p_2\,\cos(\theta - \varphi)\,\varphi' + p_1}{p_3\,p_1 - p_2^2\,\cos^2(\theta - \varphi)}. \tag{22}$$

Moreover, multiplying (7) by $\beta_2(\theta)$ and subtracting (8) multiplied by $\beta_1(\theta)$, one can observe that for this particular interval $[t_0, t_1]$, the further identity should hold $\beta_1(\theta_\star(t))\gamma_2(\theta_\star(t)) - \beta_2(\theta_\star(t))\gamma_1(\theta_\star(t)) = 0$. It gives the following differential equation for φ:

$$\varphi''(\theta) = -p_2\,\sin(\theta - \varphi(\theta)) \times \frac{p_5\,\sin(\varphi(\theta))\,(\varphi'(\theta))^2 - p_4\,\sin(\theta)}{p_5\,\sin(\varphi(\theta))\,p_2\,\cos(\theta - \varphi(\theta)) - p_4\,\sin(\theta)\,p_3}. \tag{23}$$

Similarly, the identity $\alpha_1(\theta_\star(t))\gamma_2(\theta_\star(t)) - \alpha_2(\theta_\star(t))\gamma_1(\theta_\star(t)) = 0$ is valid for $t \in [t_0, t_1]$, which gives the first-order equation

$$\varphi'(\theta) = \frac{p_5\,\sin(\varphi(\theta))\,p_1 - p_4\,\sin(\theta)\,p_2\,\cos(\theta - \varphi(\theta))}{p_5\,\sin(\varphi(\theta))\,p_2\,\cos(\theta - \varphi(\theta)) - p_4\,\sin(\theta)\,p_3}. \tag{24}$$

It can also be deduced directly combining (22) and (23).

It can be verified that under the assumption that ψ and the initial conditions for the limit cycle are sufficiently small, the right-hand side of (24) is positive, which is in contradiction with the obvious physical intuition fact that φ' should be negative at the time of impact. Hence, Case 2 is impossible for our system and will be dropped from the consideration.

The earlier arguments can be summarized as a new procedure to find limit cycles for symmetric gaits of the passive compass-gait biped as described in Problem 2.

[7]Multiply (7) by $\alpha_2(\theta)$ and subtract (8) multiplied by $\alpha_1(\theta)$ to obtain (19); for (20), multiply (7) by $\beta_2(\theta)$, and subtract (8) multiplied by $\beta_1(\theta)$.

APPENDIX
ENERGY-LIKE FUNCTION

Multiplying (14) by the scalar integrating factor $\mu(\theta)$ yields $\mu(\theta)\alpha(\theta)\,\ddot{\theta} + \mu(\theta)\beta(\theta)\,\dot{\theta}^2 + \mu(\theta)\gamma(\theta) = 0$.

Let us rewrite it in the form of Lagrangian dynamics as

$$\frac{d}{dt}\left[\frac{\partial \mathcal{L}(\theta,\dot{\theta})}{\partial \dot{\theta}}\right] - \frac{\partial \mathcal{L}(\theta,\dot{\theta})}{\partial \theta} = 0$$

with the Lagrangian given by $\mathcal{L}(\theta,\dot{\theta}) = 1/2(M(\theta)\,\dot{\theta}^2) - V(\theta)$ and the total energy being $E_x(\theta,\dot{\theta}) = 1/2(M(\theta)\,\dot{\theta}^2) + V(\theta)$, where $M(\theta) = \mu(\theta)\alpha(\theta)$ and $V(\theta) = \int_x^\theta \mu(\tau)\gamma(\tau)\,d\tau$.

It follows that

$$\frac{d}{dt}\left(\mu(\theta)\alpha(\theta)\dot{\theta}\right) + \mu(\theta)\gamma(\theta) = 0$$

and

$$\mu(\theta)\alpha(\theta)\ddot{\theta} + (\mu(\theta)\alpha'(\theta) + \mu'(\theta)\alpha(\theta))\,\dot{\theta}^2 + \mu(\theta)\gamma(\theta) = 0$$

which defines the equation for the coefficient $\mu(\theta)\beta(\theta) = \mu(\theta)\alpha'(\theta) + \mu'(\theta)\alpha(\theta)$. After separating the variables and integrating over θ, we get

$$\mu(\theta) = \frac{\alpha(x)\mu(x)}{\alpha(\theta)}\exp\left\{\int_x^\theta \frac{\beta(\tau)}{\alpha(\tau)}\,d\tau\right\}.$$

Substituting $\mu(\theta)$ (with $\mu(x)\alpha(x) = 1$) into the energy expression yields (15).

APPENDIX
RIGHT-HAND SIDE FOR THE MAIN PROCEDURE

$$\begin{aligned} f_0(a,b,\theta,\varphi(\theta),\varphi'(\theta)) = {} & (-2(-p_2(\varphi'(\theta))(\varphi'(\theta)+1)\cos(\theta-\varphi(\theta)) \\ & + p_1 + p_3(\varphi'(\theta))^3)\big(p_4 + E_0 - p_5 + p_5\cos(\varphi(\theta)) \\ & -p_4\cos(\theta))p_2\sin(\theta-\varphi(\theta)) - (-p_2(p_5\sin(\varphi(\theta))\varphi'(\theta) \\ & + p_4\sin(\theta))\cos(\theta-\varphi(\theta)) + p_5\sin(\varphi(\theta))p_1 \\ & + p_3 p_4(\varphi'(\theta))\sin(\theta))(p_1 - 2p_2\cos(\theta-\varphi(\theta))\varphi'(\theta) \\ & + p_3(\varphi'(\theta))^2))/(2(p_3 p_1 - {p_2}^2(\cos(\theta-\varphi(\theta)))^2) \\ & \times (p_4 + E_0 - p_5 + p_5\cos(\varphi(\theta)) - p_4\cos(\theta))) \end{aligned}$$

with $E_0 = E_0(a,b)$ given in (18).

REFERENCES

[1] Y. Aoustin and A. Formal'sky, "Design of reference trajectory to stabilize desired nominal cyclic gait of a biped," in *Proc. the Int. Workshop Robot Motion Control*, Kiekrz, Poland, Jun. 1999, pp. 159–165.

[2] F. Asano and Z.-W. Luo, "Asymptotically stable gait generation for biped robot based on mechanical energy balance," presented at the IEEE/RSJ Int. Conf. Intell. Robots Syst., San Diego, CA, Nov. 2007.

[3] D. Bainov and P. Simeonov, *Systems With Impulse Effects: Stability, Theory and Application* (Mathematics and Its Applications). Chichester, U.K.: Ellis Horwood, 1989.

[4] S. Collins, A. Ruina, R. Tedrake, and M. Wisse, "Efficient bipedal robots based on passive dynamic walkers," *Sci. Mag.*, vol. 307, pp. 1082–1085, 2005.

[5] L. Freidovich, A. Shiriaev, and I. Manchester, "Stability analysis and control design for an underactuated walking robot via computation of a transverse linearization," in *Proc. the 17th IFAC World Congr.*, Seoul, Korea, Jul. 2008, pp. 10 166–10 171.

[6] M. Garcia, A. Chatterjee, A. Ruina, and M. Colenman, "The simplest walking model: Stability, complexity, and scaling," *ASME J. Biomed. Eng.*, vol. 120, no. 2, pp. 281–288, 1998.
[7] D. Gates, J. Su, and J. Dingweil, "Possible biomedical origins of the long-range correlations in stride intervals of walking," *Phys. A*, vol. 380, pp. 259–270, 2007.
[8] A. Goswami, B. Espiau, and A. Keramane, "Limit cycles in a passive compass gait biped and passivity-mimicking control laws," *J. Auton. Robots*, vol. 4, no. 3, pp. 273–286, 1997.
[9] A. Goswami, B. Thuilot, and B. Espiau, "A study of the passive gait of a compass-like biped robot," *Int. J. Robot. Res.*, vol. 17, no. 12, pp. 1282–1301, 1998.
[10] J. Grizzle, G. Abba, and F. Plestan, "Asymptotically stable walking for biped robots: Analysis via systems with impulse effects," *IEEE Trans. Autom. Control*, vol. 46, no. 1, pp. 51–64, Jan. 2001.
[11] J. Hass, J. Herrmann, and T. Geisel, "Optimal mass distirbution for passivity-based bipedal robots," *Int. J. Robot. Res.*, vol. 25, no. 11, pp. 1087–1098, 2006.
[12] K. Hirata and H. Kokame, "Stability analysis of linear systems with state jump—Motivated by periodic motion control of passive walker," in *Proc. IEEE Conf. Control Appl.*, Istanbul, Turkey, Jun. 2003, pp. 949–953.
[13] I. Hiskens, "Stability of hybrid system limit cycles: Application to the compass gait biped robot," in *Proc. 40th IEEE Conf. Decision Control*, Orlando, FL, Dec. 4–7, 2001, pp. 774–779.
[14] D. Hobbelen and M. Wisse, "A disturbance rejection measure for limit cycle walking: The gait sensitivity norm," *IEEE Trans. Robot.*, vol. 23, no. 6, pp. 1213–1224, Dec. 2007.
[15] Y. Hurmuzlu and D. Marghitu, "Rigid body collisions of planar kinematic chains with multiple contact points," *Int. J. Robot. Res.*, vol. 13, no. 1, pp. 82–92, 1994.
[16] A. Kuo, "Stabilization of lateral motion in passive dynamic walking," *Int. J. Robot. Res.*, vol. 18, no. 9, pp. 917–930, 1999.
[17] A. Kuo, "Choosing your steps carefully: Trade offs between economy and versatility in dynamic walking bipedal robots," *IEEE Robot. Autom. Mag.*, vol. 14, no. 2, pp. 18–29, Jun. 2007.
[18] N. Liu, J. Li, and T. Wang, "Passive walking that can walk down steps: Simulation and experiments," *Acta Mech. Sin.*, vol. 24, pp. 569–573, 2008.
[19] T. McGeer, "Passive dynamic walking," *Int. J. Robot. Res.*, vol. 9, no. 2, pp. 62–82, 1990.
[20] A. Safa, M. Saadat, and M. Naraghi, "Passive dynamic of the simplest walking model: Replacing ramps with stairs," *Mech. Mach. Theory*, vol. 42, pp. 1314–1325, 2007.
[21] A. Shiriaev, L. Freidovich, and I. Manchester, "Can we make a robot ballerina perform a pirouette? Orbital stabilization of periodic motions of underactuated mechanical systems," *Annu. Rev. Control*, vol. 32, no. 2, pp. 200–211, 2008.
[22] A. Shiriaev, J. Perram, and C. Canudas-de Wit, "Constructive tool for orbital stabilization of underactuated nonlinear systems: Virtual constraints approach," *IEEE Trans. Autom. Control*, vol. 50, no. 8, pp. 1164–1176, Aug. 2005.
[23] A. Shiriaev, J. Perram, A. Robertsson, and A. Sandberg, "Periodic motion planning for virtually constrained Euler–Lagrange systems," *Syst. Control Lett.*, vol. 55, pp. 900–907, 2006.
[24] M. Spong and F. Bullo, "Controlled symmetries and passive walking," *IEEE Trans. Autom. Control*, vol. 50, no. 7, pp. 1025–1031, Jul. 2005.
[25] M. Spong, J. Holm, and D. Lee, "Passivity-based control of bipedal locomotion," *IEEE Robot. Autom. Mag.*, vol. 14, no. 2, pp. 30–40, Jun. 2007.
[26] E. Westervelt, J. Grizzle, C. Chevallereau, J. Choi, and B. Morris, *Feedback Control of Dynamic Bipedal Robot Locomotion*. Boca Raton, FL/New York: CRC/Taylor & Francis, 2007.
[27] E. Westervelt, J. Grizzle, and D. Koditschek, "Hybrid zero dynamics of planar biped walkers," *IEEE Trans. Autom. Control*, vol. 48, no. 1, pp. 42–56, Jan. 2003.
[28] E. Westervelt, B. Morris, and K. Farrell, "Sample-based hzd control for robustness and slope invariance of planar passive bipedal gaits," *Auton. Robots*, vol. 23, pp. 131–145, 2007.

Improving the Human–Robot Interface Through Adaptive Multispace Transformation

Luis M. Muñoz and Alícia Casals, *Senior Member, IEEE*

***Abstract*—Teleoperation is essential for applications in which, despite the availability of a precise geometrical definition of the working area, a task cannot be explicitly programmed. This paper describes a method of assisted teleoperation that improves the execution of such tasks in terms of ergonomics, precision, and reduction of execution time. The relationships between the operating spaces corresponding to the human–robot interface triangle are analyzed. The proposed teleoperation aid is based on applying adaptive transformations between these spaces.**

***Index Terms*—Human factors, human–robot interaction, teleoperation.**

I. Introduction

Teleoperation relies on a suitable interface that enables a human to provide robots with the level of intelligence needed to execute complex tasks that cannot be performed by a robot alone or directly by a human.

Humans have inherent motor limitations (such as physiological tremor) and perceptive limitations (mainly perception of distance and time), which can prevent them from operating smoothly and precisely enough for certain applications. Some studies have already tackled this problem and its effect on the control of teleoperated systems. Psychomotor models such as those defined in Fitts' law [1] show that the efficiency of human manipulation in the selection of an object depends on its size and distance.

In teleoperation, a modification of the visual scale in the user's interface has a direct effect on the task execution time and on the precision that can be achieved. The same occurs with a change in the amplitude of the movement executed in the working space with respect to that performed by the human operator. The introduction of velocity scaling maps between the master and the slave is also efficient in reducing the task execution time [2].

This paper describes a method conceived to improve the visual and motor performances of teleoperation interfaces through progressive changes of scale between the different working spaces. Operation time, hand movements, and the need for visual attention can thus be reduced. The changes of scale adapt to the application, which positively affects the performance of a task in terms of precision and execution time. Therefore, the proposed methodology aims to link the human operator working space to the robot working space through an interface that introduces two scaling processes. A first change of scale is applied between the movement produced by the human operator and the virtual position of the robot end-effector (EE) that is visualized on the computer screen. A second change scales the robot movements up or down. These changes of scale should be adjusted to the objects of interest, which results in a modification of spatial resolution according to the task to be performed and to the size and shape of the objects. Such transformations modify the manipulator speed and, thus, improve performance. Compared with other teleoperated systems, which either

Manuscript received November 18, 2008; revised April 2, 2009 and May 21, 2009. First published June 30, 2009; current version published October 9, 2009. This paper was recommended for publication by Associate Editor C. Cavusoglu and Editor K. Lynch upon evaluation of the reviewers' comments.

L. M. Muñoz is with the Universitat Politècnica de Catalunya, Barcelona 08028, Spain (e-mail: luis.miguel.munoz@upc.edu).

A. Casals is with the Institute for Bioengineering of Catalonia, Barcelona 08028, Spain (e-mail: alicia.casals@upc.edu).

Color versions of one or more of the figures in this paper are available online at http://ieeexplore.ieee.org.

Digital Object Identifier 10.1109/TRO.2009.2024790